Taylor & Francis
Taylor & Francis Group

Artificial Cells, Nanomedicine, and Biotechnology
An International Journal

ISSN: 2169-1401 (Print) 2169-141X (Online) Journal homepage: https://www.tandfonline.com/loi/ianb20

Preparation of MC3T3-E1 cell sheets through short-term osteogenic medium application

Atakan Tevlek, Sedat Odabas, Ekin Çelik & Halil Murat Aydin

ARTIFICIAL CELLS, NANOMEDICINE, AND BIOTECHNOLOGY
2018, VOL. 46, NO. S2, S1145–S1153
https://doi.org/10.1080/21691401.2018.1481081

Preparation of MC3T3-E1 cell sheets through short-term osteogenic medium application

Atakan Tevlek[a], Sedat Odabas[b], Ekin Çelik[c] and Halil Murat Aydin[d]

[a]Bioengineering Division, Institute of Science, Hacettepe University, Ankara, Turkey; [b]Department of Chemistry, Faculty of Science, Ankara University, Ankara, Turkey; [c]Bioengineering Division and Advanced Technologies Application and Research Centre, Institute of Science, Hacettepe University, Ankara, Turkey; [d]Environmental Engineering Department and Bioengineering Division and Centre for Bioengineering, Hacettepe University, Ankara, Turkey

ABSTRACT

Cell sheet engineering is an emerging field based on the acquisition of cells together with their extracellular matrix (ECM) and is used not only *in vitro* but also in regeneration studies of various tissues in the clinic. Within this scope, wide variety of cell types have been investigated in terms of sheet formation and underlying mechanism. MC3T3-E1 is a mouse pre-osteoblast cell line that has greatly attracted researchers' attention for bone tissue engineering (BTE) applications thanks to its high proliferation and differentiation properties. The potential of MC3T3-E1 cells on sheet formation and the effects of culture conditions have not been investigated in detail. This study aims to examine the effects of growth and osteogenic medium on cell sheet formation of MC3T3-E1. As a result of this study; intact, ECM-rich, transferable cell sheets at the beginning of the mineralization phase of the differentiation process were obtained by using osteogenic medium. Hereafter, 3D tissue model can be constructed by stacking MC3T3 cell sheets *in vitro*. This 3D model can conveniently be used for the development of novel biomaterials and *in vitro* drug screening applications to reduce the need for animal experiments.

ARTICLE HISTORY
Received 9 March 2018
Accepted 18 May 2018

KEYWORDS
Cell sheet; MC3T3-E1 pre-osteoblast cells; osteogenic medium; osteogenic differentiation

Introduction

Tissue engineering and regenerative medicine have been an emerging field that covers combinational therapies using cells, biomolecules and 3D materials [1]. Cell loss after direct cell injection and the failure of following direct therapeutic effects lead the researchers to discover new therapeutic strategies in regenerative medicine. After the launch of scaffold-based approaches, a vast number of studies have been carried out to create a cell-carrier. Several materials namely natural and synthetic polymers, metals, ceramics or combinations thereof have been proposed for tissue engineering applications [2]. In spite of being a tissue equivalent and having great properties, scaffolds have some disadvantages such as insufficient cell migration, host inflammatory reactions, transport problems due to the absence of vascular network, inability to harmonize with the architecture complexity of native tissues and non-tunable mechanical or degradation properties [3–5]. Therefore, bottom-up tissue engineering approaches have been proposed to overcome the limitations of scaffold-based therapies and to improve the features of scaffolds [6].

Cell sheet engineering is one of the promising bottom-up tissue engineering methods proposed by Okano et al. for the first time in the literature in 1993 [7]. A cell sheet can be defined as a monolayer, consisting of cells extracellular matrix, ion channels, growth factor receptors and other important cell surface proteins [8].

According to this technique, a temperature responsive smart polymer, poly(N-isopropyl acrylamide) (PNIPAAm), was coated on to the culture dishes at nanometre scale to obtain cell sheets via the conformational changes based on temperature differences. Hydrophobic nature of the polymer exhibits hydrophilic character explicitly as the temperature decreases below 32 °C [9]. In addition to temperature reduction method, various techniques have been proposed to fabricate cell sheets up to date: enzymatic treatment, magnetic force application, electrochemical polarization, U.V. inducement, hexacyanoferrate (II)-induced dissolution, electrochemically induced pH decrease, mechanical retrieval and Vitamin-C treatment [10–17]. Various cell types, from primary cells to mesenchymal stem cells have been examined since the discovery of cell sheet engineering in terms of not only sheet formation but also obtaining multi-layered cell sheets and 3D tissues [18]. Obtained cell sheets have been successfully used in clinic or have been suggested for repairing several tissues *in vitro* or *in vivo* such as oesophagus [19], myocardium [20], bone [21], cornea [22], blood vessels [23] and periodontal tissue [24].

MC3T3-E1 mouse pre-osteoblast cell line is a widely used cell type for bone tissue engineering (BTE). Representation of the pre-osteoblastic phenotype during culture period, high

CONTACT Halil Murat Aydin hmaydin@hacettepe.edu.tr Environmental Engineering Department and Bioengineering Division and Centre for Bioengineering, Hacettepe University, Ankara 06800, Turkey

proliferation and differentiation capacity, Type-I collagen synthesis and ALP enzyme activity from day 3 in culture period, demonstration of mineralization in the presence of ascorbic acid and inorganic phosphate etc. are among the attractive properties of these cells [25–27]. Even though these properties have paved the way for these cells to become one of the ideal candidate in respect of cell source for *in vitro* BTE studies, MC3T3-E1 cells have not investigated effectively in cell sheet engineering studies.

In this study, whether MC3T3-E1 cells formed into an intact, transferable cell layers under different culture conditions were investigated. Briefly, equal amount of cells were seeded on Nunc Upcell^{TM} Petri dishes and cultured for 10 d by using growth and osteogenic medium. Attachment and detachment success of the obtained sheets were examined. Also, extracellular matrix (ECM) formation was studied related to differentiation capacity of the cells at pre-determined time points and cell sheet qualities were discussed with regard to the ECM synthesis. Differentiation was confirmed by using Real-Time PCR analyses. Besides, Alizarin Red staining, collagen and GAG quantification studies were conducted in order to reveal the Ca^{2+} and ECM quantity in the cell sheets.

Materials and methods

Cell line and maintenance

MC3T3-E1 mouse pre-osteoblast cell line Sub clone 4 (ATCC® CRL-2593^{TM}, Manassas, VA) was obtained and expanded in Alpha Minimum Essential Medium (MEM-α) supplemented with 10% FBS (*v/v*), 2 mM L-glutamine, penicillin/streptomycin (100 unit/mL penicillin-100 L/mL streptomycin). Passage 19–20 cells were used during the cell culture study. 1×10^6 cells/Nunc Up cell Petri dish (8.8 cm^2 surface area, 35 mm petri dish) was determined as seeding density to obtain cell sheets. Cells were cultured in both growth medium and osteogenic differentiation medium for 10 d until they reach over-confluency. For differentiation group, culture medium replaced after 24 h with differentiation medium containing 10 mM β-glycerol phosphate and 50 μg/mL L-ascorbic acid. For each group, culture medium was replenished with the preheated fresh one in every 3–4 d.

Preparation of cell sheets

According to the manufacturer guidelines, detachment and attachment processes were followed respectively. After 10 d of incubation process, culture media was removed from the wells. Then, wells were washed with 1 mL Dulbecco's phosphate buffer saline (D-PBS) pre-heated to 37 °C to remove the dead cells. After aspirating the D-PBS, 50 μL fresh medium pre-heated to room temperature was added to prevent the cells from drying. Afterwards, transfer membranes were placed on top of the cell layer with the help of forceps and border of the cell sheet was interrupted with a sharped-tipped surgical blade. Subsequently, well plates were kept in an incubator set to 20 °C for 20 min. At the end of the incubation period, cell sheets were detached from the Nunc Up^{TM} cell surface. The transfer membranes including cell sheets were transferred to a six-well plate's surface incubated with 1 mL FBS through overnight.

Characterization studies

Imaging techniques

Detachment and attachment efficacy of the cell sheets were investigated by an inverted microscope (Leica, Wetzlar, Germany). The remnant cells on the Nunc Upcell^{TM} surface after detachment were stained with 10% EverBrite^{TM} hardset mounting medium with DAPI (4′,6-diamidino-2-phenylindole) (Biotium, Fremont, CA) for 1 h in an incubator at 37 °C while the attached cell sheets were displayed with bright field imaging technique.

Sulphated glycosaminoglycan (sGAG) quantification

Dimethyl methylene blue (DMMB) (Sigma-Aldrich, Munich, Germany) assay was performed to quantify sulphated glycosaminoglycan (sGAG) content related to formed ECM of the cultured cells in both growth medium and osteogenic medium. Samples were digested with 1 mg/mL Proteinase K (Sigma-Aldrich, Munich, Germany) in 100 mM ammonium acetate (Merck, Darmstadt, Germany) solution at 60 °C for 15 min. Cell lysate was mixed with DMMB reagent solution (40 mmol/L sodium chloride, 40 mmol/L glycine, 46 μmol/L DMMB and 0.1 M hydrochloride) and absorbance of the mixture was recorded at 525 nm immediately by using a spectrophotometer (Spectrostar Nano, BMG Labtech, Ortenberg, Germany). An aliquot of 0–50 μg/mL standards were prepared by dissolving chondroitin sulphate from bovine cartilage (Sigma-Aldrich, Gillingham, UK) in PBS to calculate the quantity of GAG.

Calcium quantification and Alizarin Red staining

Calcium quantities of the sheets were studied by cetylpyridinium chloride (CPC) and formed calcium particles were stained with Alizarin Red-S (Sigma-Aldrich, Munich, Germany). Briefly, medium was discarded from each well and the wells were washed with PBS twice. Then, cells were fixed with 70% (*v/v*) EtOH for 1 h. Following the fixation, cell sheets were rinsed with distilled water twice. Afterwards, 1% (*w/v*) Alizarin Red aqueous solution at pH 4.2 was applied to each sample for 20 min at room temperature on an orbital shaker. At the end of the incubation time, samples were washed with distilled water five times. Lastly, PBS washing was applied for 20 min to remove nonspecific staining. The stained cell sheets were observed under a phase contrast microscope with a digital camera (Leica, Wetzlar, Germany). After imaging, cells were de-stained with 1 mL of 10% (*w/v*) CPC (Sigma-Aldrich, Munich, Germany) prepared in 10 mL of sodium phosphate (10 mM and pH 7) for 15 min with gentle rotation at room temperature. Afterwards, 200 μL of samples were collected from the wells as three parallels and were read at 562 nm by using a microplate reader (BioTek, Potton, UK). A standard curve was prepared by combining different amount of Alizarin Red stock solution with 10% (*w/v*) CPC solution. The concentration of Alizarin Red staining was determined by comparing the absorbance values with standard curve.

Collagen quantification

Collagen quantities of the cell sheets were examined with Hydroxyproline Colorimetric Assay Kit (BioVision, Milpitas, CA). Briefly, culture medium was discarded from each well. Then, samples were washed with PBS twice. To extract the hydroxyproline amino acid, 100 µL ultrapure water and 12 N hydrochloric acid (HCl) were added to the petri dishes an incubated at 120 °C for 3 h to homogenize the cell sheets. At the end of the incubation period cell lysates were centrifuged at 10,000 rpm for 3 min to obtain the supernatant and the precipitate. Overall, 50 µL supernatants were added to 96 well plate as three parallel and dried under the fume hood for overnight. An aliquot of 100 µL chloramine T was added onto the dried samples and incubated at room temperature for 5 min. Then, 100 µL p-dimethylaminobenzaldehyde (DMAB) was added and incubated at 60 °C for 90 min. Absorbance of hydroxyproline was recorded by using a microplate reader (BioTek, Potton, UK) at 560 nm.

Quantitative-PCR studies

Obtained cell sheets were stored at −80 °C until the day that RT-PCR studies perform. Samples were homogenized in lysis buffer (Next Advance Homogenizer, Troy, NY) for a minute prior to RNA extraction that was performed according to the manufacturer's instructions (Quick RNA MiniPrep RNA Isolation Kit, Zymo Research, Irvine, CA). Isolated RNAs were then transcribed by using High Capacity Reverse Transcription Kit (Thermo Fisher Scientific, Waltham, MA) with the specific primers at 25 °C for 10 min, at 37 °C for 120 min and 85 °C for 5 min in 20 µL, respectively. Gene expression studies were performed by using Viia7 Real-Time PCR System (Thermo Fisher Scientific, Waltham, MA) with PowerUp SYBR Green Master Mix and the specific primers. Collagen Type I (*Coll1*), Runt-related transcription factor 2 (*Runx2*), alkaline phosphatase (*ALP*), Osteocalcin (*Ocn*) and Osteopontin (*Opn*) genes were examined and *β-Actin* (β-Act) was used as "Housekeeping Gene" (Oligomer, Ankara, Turkey). Genes and related primers are listed in Table 1. Subsequently, comparative Ct (ddCT) values were recorded. Efficiency of primers used in this study was checked via OligoAnalyzer Tool (IDT, Newark, New Jersey). Primers were used in 10 nM concentrations in 20 µL that contains 4 µL sample.

Table 1. Genes and related primers used within the study.

Genes	Primers
B-Actin	F-GTGCTATGTTGCCCTAGACTTCG R-GATGCCACAGGATTCCATACCC
Col1A1	F-CAAGATGTGCCACTCTGACT R-TCTGACCTGTCTCCATGTTG
Runx2	F-GCATGGCCAAGAAGACATCC R-CCTCGGGTTTCCACGTCTC
ALPL	F- GGAGATGGTATGGGCGTCTC R- GGACCTGAGCGTTGGTGTTA
Ocn	F-CTTTCTGCTCACTCTGCTG R-TATTGCCCTCCTGCTTGG
Opn	F-CACTTTCACTCCAATCGTCCCTAC R-ACTCCTTAGACTCACCGCTCTTC

Statistical analyses

The number of samples for each method was set to three. Student T-test was performed to determine the statistical differences between the groups by using GraphPad Prism software version 6 (GraphPad Software, La Jolla, CA). p values at least less than .05 were considered significant in each experiment. Different p values and their level of significance are represented in detail in each figure.

Results

Effects of culture conditions on obtaining cell sheet

Cell morphology changes were observed by the end of third day of culture (data not shown) and representative images of cells at day-10 incubated with growth media and osteogenic media are given in Figure 1. Both cuboidal and star-shaped morphology were observed in growth medium (Figure 1(A)) while elongated spindle-shaped cell morphology was observed in osteogenic medium (Figure 1(B)). These morphological changes are consequences of the presence of ascorbic acid and β-glycerol phosphate supplemented to the culture medium and were deemed as the first indicator of cell differentiation.

Detachment and attachment efficacy of cell sheets

Detachment and attachment success of the cell sheets were observed by using DAPI staining and light microscopy observation and the representative images are given in Figure 2. For this purpose, all images were recorded from the middle of the well plates to discuss the sheet integrity. The detachment of the cells from the plate surface was found inadequate in the group of growth medium at the optimized circumstances. A large quantity of cells adhered to the surface that deteriorate the sheet integrity was observed. On the other hand, it was observed that the cells that stuck on the surface were in clusters and caused the undesirable sheet formation (Figure 2). It was inevitable that the cell sheets obtained through only growth medium application were curling and folded on themselves. As a result, this application did not meet the major expectations such as being easy to be carried, seamlessly transferrable from well plate to another surface and applied practically. The resulting macroscopic images from the wells after cell sheet attachment can be seen as evidence to this situation (Figure 3).

When it comes to evaluate the effects of osteogenic medium application on cell sheet formation, detachment success was remarkable as understood from the images obtained with DAPI staining (Figure 2). Only a few cells in spherical form, indicative of metabolically inactive or dead cells, were observed on the thermo-responsive surface. Both microscopic and macroscopic images regarding the attached cell sheets on a well of six well-plate (Figures 2 and 3(B), respectively) were confirmed the success of osteogenic medium

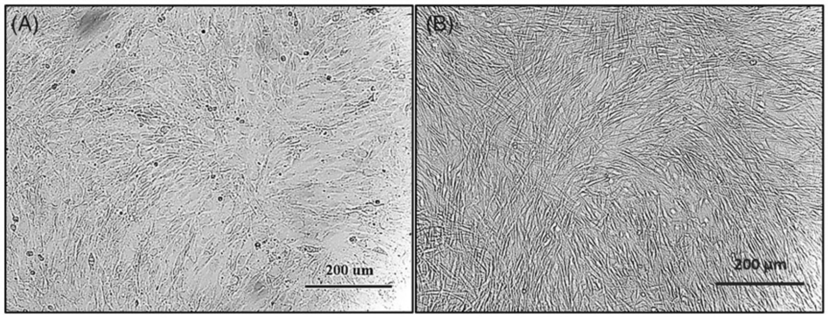

Figure 1. Morphology of the cells at day-10 cultured with different conditions: (A) Growth Medium and (B) Osteogenic Medium.

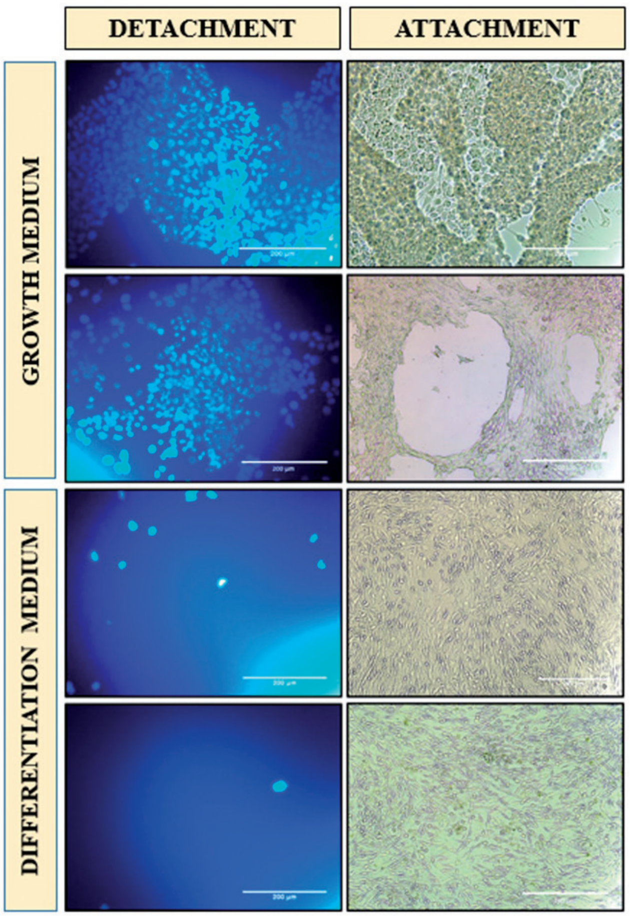

Figure 2. Detachment and attachment success of the cell sheets obtained by using growth medium and osteogenic medium.

application on sheet integrity. Additionally, the differences of cell morphology can be clearly seen from the microscopic images of different transferred cell sheets obtained through growth medium and osteogenic medium (Figure 2). This confirms the variation of cell morphology due to cell differentiation seen in Figure 1.

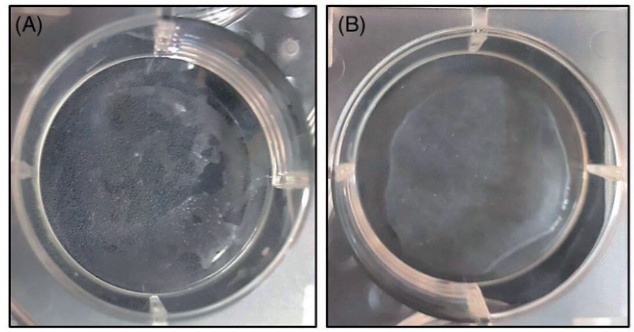

Figure 3. Macroscopic comparison of cell sheet integrity: (A) Growth medium and (B) Osteogenic medium.

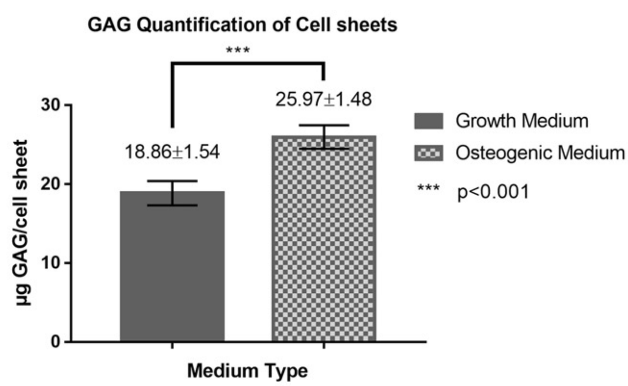

Figure 4. GAG quantification of cell sheets obtained through growth and osteogenic medium application.

Sulphated-glycosaminoglycan (GAG) quantification

GAG quantity of the cell sheets was measured by DMMB assay to reveal the ECM formation of cultured cells with growth and osteogenic medium. Results are given as µg/cell sheet by using a standard curve derived from chondroitin sulphate solution in PBS. Results are shown that the cell sheets obtained through the osteogenic medium application have 25.97 ± 1.48 µg, while other cell sheets resulting from the addition of growth medium have 18.86 ± 1.54 µg GAG content. The cell sheets obtained through osteogenic medium has approximately 1.4 times higher GAG content than the former (Figure 4).

Collagen quantification

Collagen depositions in the cell sheets quantified by hydroxyproline assay are given in Figure 5. The increase in secreted collagen was remarkable in the cell sheets obtained by osteogenic medium application ($p < .0001$). The collagen accumulation in the cell sheets formed by the cells cultured with the growth medium was measured as 0.022 ± 0.011 µg while the collagen deposition in the cell sheets formed by the cells cultured with the osteogenic medium was measured as 0.215 ± 0.022 µg. It was observed that the use of osteogenic medium increases the collagen deposition by around 10-fold.

Real time-PCR studies

The results of real-time quantitative gene expression analysis are given in Figure 6. The expression level of *Col1A1*, *ALPL*, *Runx2*, *Ocn* and *Opn* were analyzed and their effects on sheet formation were discussed in detail.

Two different time points were studied to understand the mechanism of sheet formation with osteogenic medium. The main purpose of the different time point selection is to compare the results with the previous studies in the literature with regards to β-glycerol phosphate and L-ascorbic acid addition. It was revealed that *Col1A1*, *ALPL* and *Ocn* genes were upregulated in the presence of β-glycerol phosphate and L-ascorbic acid ($p < .001$ for all) at 10th day of the culture period. On the fifth day of culture, there was no significant difference between the two groups in terms of *Col1A1* expression. At later stages of culture, upregulation of *Col1A1* was observed when comparing with the fifth day of culture in osteogenic medium group ($p < .5$). The decrease in *Col1A1* expression in the growth medium group was due to most probably the high amount of cell loss during the cell sheet preparation stage as stated in Figures 2 and 3. The same situation was encountered when the expression levels of other genes were examined, reinforcing our hypothesis. On the fifth day of culture; there was no difference between the two groups in terms of *ALPL* expression (Figure 6). But on the last day of the culture period, *ALPL* expression of the cell sheet obtained through osteogenic medium was found approximately 1.5 times greater than the cell sheets incubated with growth medium for 5 d (Figure 6).

For the *Runx2* expression, there was no difference between the two groups in the presence of β-glycerol phosphate and L-ascorbic acid when compared with the initial phase of the culture period (Figure 6). It was thought that the differences in the expression level of *Runx2* of the obtained cell sheets were occurred due to the cell loss. The absence of *Runx2* expressions could have stemmed from the special organization of the genes during the osteogenic differentiation and was evaluated in the discussion session. On the contrary of *Runx2*, *Ocn* was found upregulated in the group that used osteogenic medium ($p < .001$). It was found that *Ocn* expression was approximately 1.2 times greater than the resulting cell sheets that incubated 5 d with growth medium (Figure 6). Unlike all other genes, *Opn* was observed to be upregulated in the cell sheets formed by the growth medium surprisingly when all the time points were considered ($p < .001$). Even, the expression of *Opn* was found approximately two folds higher in the sheets incubated

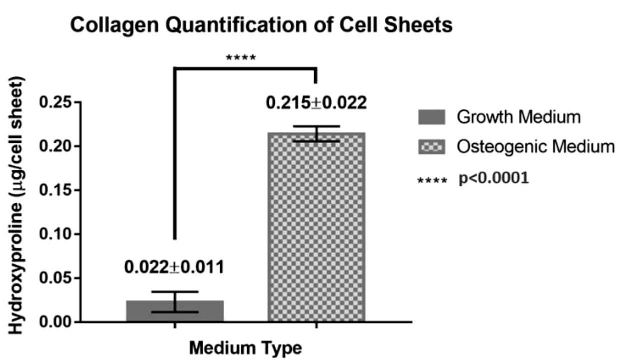

Figure 5. Collagen quantification of cell sheets obtained through growth and osteogenic medium application.

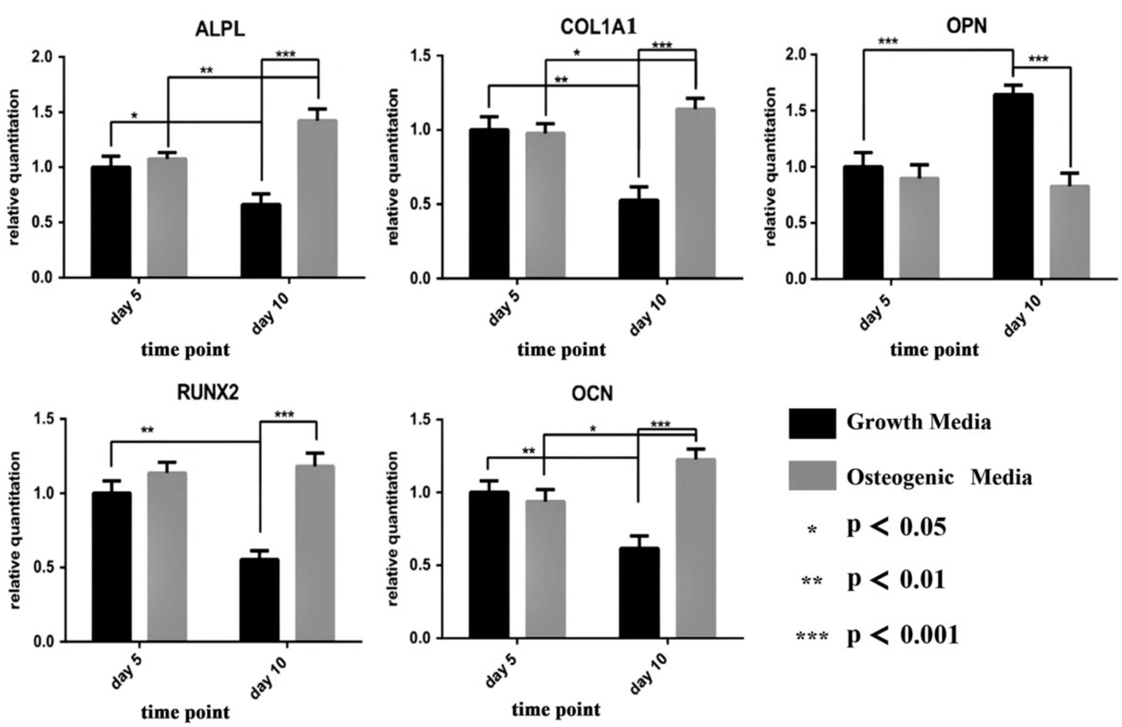

Figure 6. Comparison of osteogenic gene expression between the resulting cell sheets.

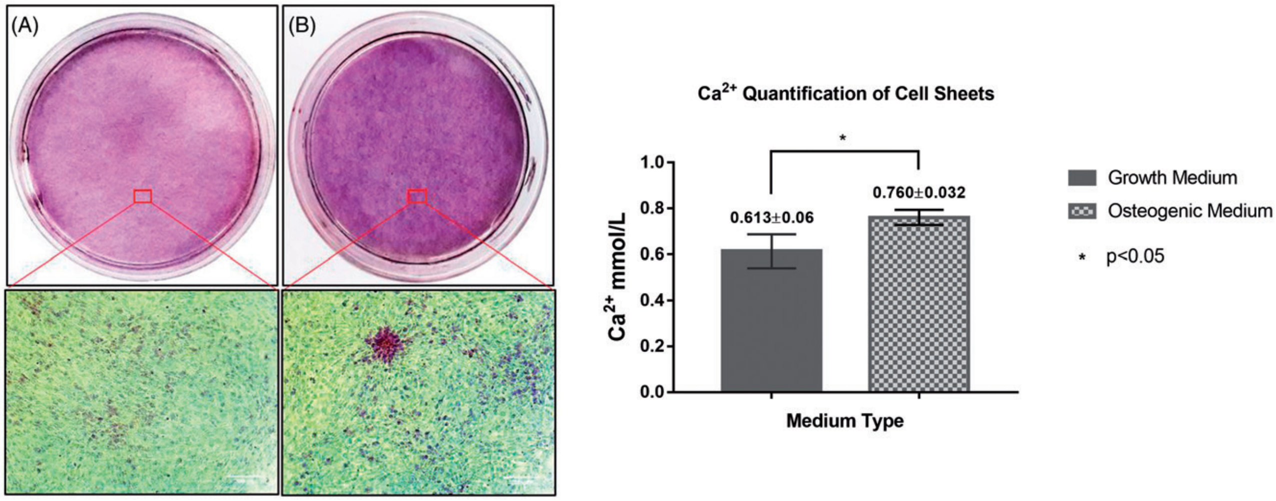

Figure 7. Alizarin Red staining and Ca^{2+} quantification of cell sheets: (A) Growth Medium and (B) Osteogenic Medium.

with growth medium at day 10 when compared to osteogenic medium.

Calcium quantification and Alizarin Red staining

Alizarin Red staining studies were performed to investigate calcium deposition and CPC assay was used to interpret the Ca^{2+} quantity by using optic density values at 562 nm with the help of CPC standard curve. Relevant images and obtained data are presented in Figure 7.

Use of osteogenic medium was provided Ca^{2+} accumulation between the cells as understood from the images in Figure 7(B). The calcium nucleation among the cells is clearly visible with red staining. The same staining was not observed in the cell sheets obtained with the growth medium. Differences in the formation of calcium in cell sheets are shown not only in Alizarin Red staining but also quantitatively (Figure 7). According to these findings, 0.760 ± 0.032 mmol/L Ca^{2+} was detected from the sheets that formed with osteogenic group while the sheets obtained from growth medium was exhibited 0.613 ± 0.06 mmol/L Ca^{2+} accumulation. Although there was a difference between the groups in terms of Ca^{2+} accumulation ($p < .5$), the values obtained were close to each other indicating the beginning of the mineralization phase. On the other hand, it was thought that the red scattered dots observed in microscopic images of cell sheets obtained through growth medium were dye residues and not related to calcium particles.

Discussion

The effects of ascorbic acid and β-glycerol phosphate on MC3T3-E1 cell line have been widely investigated since Quarles et al.'s first publication in 1992. Mineralized matrix formation via the addition of 25–50 μg/mL ascorbic acid and 5–10 mM β-glycerol phosphate to the culture medium has been reported by several researchers [25,28,29]. Within the scope of this research study, the effect of culture medium containing ascorbic acid and β-glycerol phosphate on cell sheet formation was investigated in detail.

Twenty-four hours after the addition of ascorbic acid to the culture medium, increased Type-I pro-collagen mRNA and collagen synthesis have been reported previously [30]. This situation is one of the mainstay of our hypothesis in order to obtain intact cell sheet with the help of collagen accumulation in the ECM. However, *Col1A1* expressions were found similar in both groups on the fifth day of culture indicating that the cells were still in the proliferation stage, despite the addition of osteogenic medium (Figure 6). On the other hand, a time-dependent increase was observed in the osteogenic group ($p < .5$) as opposed to the growth medium in terms of *Col1A1* expressions. The time-dependent decrease of *Col1A1* expressions in the growth medium group is thought to be due to cell death resulting from confluency.

Similarly, it has been reported that ALP and osteocalcin mRNAs were sequentially induced following collagen expression after 48–72 h and 96–144 h following the addition of ascorbic acid [30]. Choi et al. described the osteogenic differentiation in three main steps: proliferation phase that covers 4–10 d of the culture period, bone matrix formation/maturation that covers 10–16 d of the culture period and mineralization phase between the 16th and 30th days of culture period [31]. It was concluded that our quantitative PCR results were found consistent with this classification and thus a cell sheet composed of cells at the beginning of the mineralization stage was obtained and more details are given below.

While the expression of *Runx2* was evaluated, it was understood that there was no significant difference between the groups at day-10. Moreover, there was no time-dependent change in the expression of *Runx2* in any of the experimental groups. *Runx2* is a multifunctional transcription factor that is responsible for not only differentiation of osteoblasts but also expression of a good many ECM protein [32]. *Runx2* induces the expression of bone matrix protein genes of preosteoblasts and allows cells to acquire an osteoblastic phenotype. On the other hand, it allows the cells to remain in custody at the immature stage [33]. Especially, it plays a crucial role on regulation of various bone matrix genes including *Col1A1*. Hence, there is a strong correlation between these two genes. The decreased *Runx2* expression in mature osteoblasts may nevertheless be necessary for the supply of expression of *Col1A1* [34]. Accordingly, the possible cause of the absence of *Runx2* up-regulation in our results can be explained by the maintenance of active collagen expression in the osteogenic medium group.

Ocn is the most common protein found in the bone matrix after collagen [35]. Mature osteocalcin undergoes a conformational change after it was secreted into the bone microenvironment and regulates mainly the mineralization phase in differentiation process [36]. Up-regulation of osteocalcin is an indication of the transition of cells to the mineralization phase during the differentiation process. The 1.2-fold increase in *Ocn* expression observed in the osteogenic medium group (Figure 6) was interpreted as proof of osteogenic differentiation and matrix maturation. On the other hand, red stained Ca^{2+} particles and increased Ca^{2+} content in cell sheets ($p < .5$) obtained by osteogenic medium were an indication of the initiation of mineralization in the ECM. On the basis of these findings, in the group of osteogenic medium, it was predicted that when the culture period is extended, accumulation of more calcium particles in the cell layers would occur and that these calcium particles deteriorate the sheet integrity. Hence, a 10-day of culture period was found to be sufficient in order to acquire an intact cell sheet containing the cells at the beginning of the mineralization process.

On the other hand, it was noteworthy that the cell sheets obtained by using osteogenic medium in our study exhibited ALP expression 1.5 times higher ($p < .001$) than the growth medium (Figure 6). Also, there was a time-dependent increase in terms of ALP expression in the osteogenic medium group ($p < .01$). ALP is a ubiquitous cellular protein that has wide variety of responsibilities in the tissues and cannot be accepted as bone specific [37]. But, in bone tissue development process it undertakes an important task as a differentiation marker and plays a crucial role on ECM formation together with collagen expression [38]. ALP facilitates the mineralization process forming phosphate ions thanks to its phosphatase property and these phosphates bind to the calcium to form calcium-phosphate compound [39]. The high ALP expression in addition to the increased *Ocn* expression in the osteogenic group in our study was thought to play an important role in the mineralization process.

Opn is one of the non-collagenous ECM protein of mineralized tissues in a highly phosphorylated and glycosylated form and on the other hand it is found in kidneys, epithelial lining tissues, blood plasma and breast milk [40,41]. Specifically, in bone tissue, it regulates cell adhesion, cell migration and cell survival in harmony with others generally but as a late stage differentiation marker it is responsible for the regulation of mineralization. The expression of *Opn*, that can be seen either in early or late stages of osteogenic differentiation, should be interpreted differently. Huang et al. reported that *Opn* is responsible for inhibiting proliferation and differentiation of MC3T3-E1 cells [42]. Accordingly, the observation of increased *Opn* expression in the cell sheets obtained by using growth medium ($p < .001$) within this study was associated with inhibition of proliferation, depending on over-confluency (Figure 6). On the other hand, there was no significant difference between *Opn* expressions of the osteogenic medium group on the different time points of culture period. The increase in *Opn* expression in the late stages of osteogenic differentiation leads to a decrease in the expression of osteocalcin and bone sialoproteins, which means that the mineralization phase is terminated [43]. Thus, it was confirmed again that the cell sheets obtained with the osteogenic medium were still composed of cells that were in the mineralization stage.

The amount of ECM contained in the cell sheets obtained in this study was determined both by collagen quantification analysis and by measuring the amounts of GAG – the non-collagenous components of the ECM. It was observed that the osteogenic medium used in the study increased collagen synthesis and collagen was detected in the cell sheets obtained by using osteogenic medium approximately 10 times higher ($p < .0001$) (Figure 5). Likewise, it was found that the amount of glycosaminoglycans increased in the presence of osteogenic medium and that the cell sheets obtained by using osteogenic medium contained 1.4 times more GAG than those obtained by using growth medium ($p < .001$) (Figure 4). Promoted collagen synthesis and GAG accumulation by ascorbic acid administration have been previously demonstrated in the literature by Hata and Senoo [44] and Kao et al. [45], respectively. The results obtained in our study related to collagen and GAG quantification also confirm above-mentioned previous literature studies.

Similarly to our study, Wei et al. [46] investigated the effects of Vitamin C treatment on human periodontal ligament mesenchymal stem cell (hPDLSCs) sheet formation. They reported increased ECM synthesis and induced telomerase activity by using Vitamin C and proposed this technique as an easy and practical application on cell sheet formation. On the other hand, Pirraco et al. [12] reported a study based on obtaining cell sheet from rat bone marrow mesenchymal stem cells by using osteogenic medium including 10^{-8} M dexamethasone, 50 mg/mL ascorbic acid and 10 mM β-glycerol phosphate. Wong-In et al. [47] reported a new temperature responsive tissue culture surface containing poly (N-isopropylacrylamide-co-acrylamide) (PNIPAM-co-AM) and tested this surface with MC3T3-E1 cells in terms of thermo-responsive behaviour. When the macroscopic images of their cell sheet were compared with the cell sheet obtained *via* growth medium used in this study, weak sheet integrity and the presence of holes and curlings were found common.

In the above-mentioned studies, either osteogenic differentiation agents were used to obtain a cell sheet in the culture of different cell types or a new thermo-responsive surface was tested with MC3T3-E1 cells. Previously, no study to date examined the potential of MC3T3-E1 cells on sheet formation together with its underlying mechanisms in the presence of osteogenic medium. Therefore, it was considered that the findings obtained in this study will shed light on future studies related to cell sheet engineering.

Conclusion

This study offers intact MC3T3-E1 cell sheets obtained by using thermo-responsive commercial tissue culture plates (Nunc UpCell^{TM}). The effects of culture conditions on cell sheet formation and sheet quality were discussed. Thus, MC3T3-E1 cell sheet preparation together with underlying mechanism is reported. The obtained intact, ECM-rich, transferable, MC3T3-E1 cell sheets at the beginning of the mineralization phase of differentiation process can be used for further applications such as constructing into a 3D tissue model both stacking cell sheets or combination with the biomaterials. Moreover, these structures can be also used in biomaterial development, *in vitro* drug monitoring and *in vitro* models to reduce animal studies.

Acknowledgements

The authors would like to thank BMT Calsis Co. for their infrastructural support.

Disclosure statement

No potential conflict of interest was reported by the authors.

Funding

This study was supported by The Scientific and Technological Research Council of Turkey (TUBITAK) within the scope of 2211-C Priority Areas Related to Doctoral Scholarship Programme. The scholarship was granted to A. Tevlek by TUBITAK.

ORCID

Atakan Tevlek https://orcid.org/0000-0003-0601-8642
Sedat Odabas http://orcid.org/0000-0002-7844-7019

References

[1] Mao AS, Mooney DJ. Regenerative medicine: current therapies and future directions. Proc Natl Acad Sci USA. 2015;112:14452–14459.
[2] Henkel J, Hutmacher DW. Design and fabrication of scaffold-based tissue engineering. BioNanoMaterials. 2013;14:171–193.
[3] Bramfeld H, Sabra G, Centis V, et al. Scaffold vascularization: a challenge for three-dimensional tissue engineering. Curr Med Chem. 2010;17:3944–3967.
[4] Alaribe FN, Manoto SL, Motaung SCKM. Scaffolds from biomaterials: advantages and limitations in bone and tissue engineering. Biologia. 2016;71:366.
[5] Gervaso F, Sannino A, Peretti GM. The biomaterialist's task: scaffold biomaterials and fabrication technologies. Joints. 2013;1:130–137.
[6] Elbert DL. Bottom-up tissue engineering. Curr Opin Biotechnol. 2011;22:674–680.
[7] Okano T, Yamada N, Sakai H, et al. A novel recovery system for cultured cells using plasma-treated polystyrene dishes grafted with poly(N-isopropylacrylamide). J Biomed Mater Res. 1993;27:1243–1251.
[8] Chen G, Qi Y, Niu L, et al. Application of the cell sheet technique in tissue engineering (Review). Biomed Rep. 2015;3:749–757.
[9] Akiyama Y, Kikuchi A, Yamato M, et al. Ultrathin poly(N-isopropylacrylamide) grafted layer on polystyrene surfaces for cell adhesion/detachment control. Langmuir. 2004;20:5506–5511.
[10] Akahane M, Shimizu T, Kira T, et al. Culturing bone marrow cells with dexamethasone and ascorbic acid improves osteogenic cell sheet structure. Bone Joint Res. 2016;5:569–576.
[11] Gipson IK, Grill SM. A technique for obtaining sheets of intact rabbit corneal epithelium. Investig Ophthalmol Vis Sci. 1982;23:269–273.
[12] Pirraco RP, Obokata H, Iwata T, et al. Development of osteogenic cell sheets for bone tissue engineering applications. Tissue Eng A. 2011;17:1507–1515.
[13] Guillaume-Gentil O, Akiyama Y, Schuler M, et al. Polyelectrolyte coatings with a potential for electronic control and cell sheet engineering. Adv Mater. 2008;20:560–565.
[14] Guillaume-Gentil O, Semenov OV, Zisch AH, et al. PH-controlled recovery of placenta-derived mesenchymal stem cell sheets. Biomaterials. 2011;32:4376–4384.
[15] Zahn R, Thomasson E, Guillaume-Gentil O, et al. Ion-induced cell sheet detachment from standard cell culture surfaces coated with polyelectrolytes. Biomaterials. 2012;33:3421–3427.
[16] Hong Y, Yu M, Weng W, et al. Light-induced cell detachment for cell sheet technology. Biomaterials. 2013;34:11–18.
[17] Shimizu K, Ito A, Lee JK, et al. Construction of multi-layered cardiomyocyte sheets using magnetite nanoparticles and magnetic force. Biotechnol Bioeng. 2007;96:803–809.
[18] Matsuda N, Shimizu T, Yamato M, et al. Tissue engineering based on cell sheet technology. Adv Mater. 2007;19:3089–3099.
[19] Kanai N, Yamato M, Okano T. Cell sheets engineering for esophageal regenerative medicine. Ann Transl Med. 2014;2(3):2.
[20] Sawa Y, Miyagawa S. Present and future perspectives on cell sheet-based myocardial regeneration therapy. BioMed Res Int. 2013;2013:1.
[21] Long T, Zhu Z, Awad HA, et al. The effect of mesenchymal stem cell sheets on structural allograft healing of critical sized femoral defects in mice. Biomaterials. 2014;35:2752–2759.
[22] Nishida K, Yamato M, Hayashida Y, et al. Functional bioengineered corneal epithelial sheet grafts from corneal stem cells expanded ex vivo on a temperature-responsive cell culture surface. Transplantation. 2004;77:379–385.
[23] Asakawa N, Shimizu T, Tsuda Y, et al. Pre-vascularization of in vitro three-dimensional tissues created by cell sheet engineering. Biomaterials. 2010;31:3903–3909.
[24] Wang Z, Feng Z, Wu G, et al. In vitro studies on human periodontal ligament stem cell sheets enhanced by enamel matrix derivative. Colloid Surf B Biointerfaces. 2016;141:102–111.
[25] Czekanska EM, Stoddart MJ, Richards RG, et al. In search of an osteoblast cell model for in vitro research. Eur Cell Mater. 2012;24:1–17.
[26] Quarles LD, Yohay DA, Lever LW, et al. Distinct proliferative and differentiated stages of murine MC3T3-E1 cells in culture: an in vitro model of osteoblast development. J Bone Miner Res. 2009;7:683–692.
[27] Tevlek A, Hosseinian P, Ogutcu C, et al. Bi-layered constructs of poly(glycerol-sebacate)-β-tricalcium phosphate for bone-soft tissue interface applications. Mater Sci Eng C. 2017;72:316–324.
[28] Kuo ZK, Lai PL, Toh EKW, et al. Osteogenic differentiation of preosteoblasts on a hemostatic gelatin sponge. Sci Rep. 2016;6:32884.
[29] Yazid MD, Ariffin SHZ, Senafi S, et al. Determination of the differentiation capacities of murines' primary mononucleated cells and MC3T3-E1 cells. Cancer Cell Int. 2010;10:42.
[30] Franceschi RT, Iyer BS. Relationship between collagen synthesis and expression of the osteoblast phenotype in MC3T3-E1 cells. J Bone Miner Res. 2009;7:235–246.
[31] Choi JY, Lee BH, Song KB, et al. Expression patterns of bone-related proteins during osteoblastic differentiation in MC3T3-E1 cells. J Cell Biochem. 1996;61:609–618.
[32] Prince M, Banerjee C, Javed A, et al. Expression and regulation of RUNX2/Cbfa1 and osteoblast phenotypic markers during the growth and differentiation of human osteoblasts. J Cell Biochem. 2001;80:424–440.

[33] Maruyama Z, Yoshida CA, Furuichi T, et al. Runx2 determines bone maturity and turnover rate in postnatal bone development and is involved in bone loss in estrogen deficiency. Dev Dyn. 2007;236:1876–1890.

[34] Komori T. Regulation of bone development and extracellular matrix protein genes by RUNX2. Cell Tissue Res. 2010;339:189–195.

[35] Komori T, Yagi H, Nomura S, et al. Targeted disruption of Cbfa1 results in a complete lack of bone formation owing to maturational arrest of osteoblasts. Cell. 1997;89:755–764.

[36] Zoch ML, Clemens TL, Riddle RC. New insights into the biology of osteocalcin. Bone. 2016;82:42–49.

[37] Kirkham GR, Cartmell SH. Genes and proteins involved in the regulation of osteogenesis. Genes Osteogenes. 2007;3:1–22.

[38] Rutkovskiy A, Stensløkken KO, Vaage IJ. Osteoblast differentiation at a glance. Med Sci Monit Basic Res. 2016;22:95–106.

[39] Golub EE, Boesze-Battaglia K. The role of alkaline phosphatase in mineralization. Curr Opin Orthop. 2007;18:444–448.

[40] Denhardt DT, Noda M. Osteopontin expression and function: role in bone remodeling. J Cell Biochem. 1998;30–31:92–102.

[41] Standal T, Borset M, Sundan A. Role of osteopontin in adhesion, migration, cell survival and bone remodeling. Exp Oncol. 2004;26:179–184.

[42] Huang W, Carlsen B, Rudkin G, et al. Osteopontin is a negative regulator of proliferation and differentiation in MC3T3-E1 preosteoblastic cells. Bone. 2004;34:799–808.

[43] Yuan Q, Jiang Y, Zhao X, et al. Increased osteopontin contributes to inhibition of bone mineralization in FGF23-deficient mice. J Bone Miner Res. 2014;29:693–704.

[44] Hata R, Senoo H. L-ascorbic acid 2-phosphate stimulates collagen accumulation, cell proliferation, and formation of a three dimensional tissuelike substance by skin fibroblasts. J Cell Physiol. 1989;138:8–16.

[45] Kao J, Huey G, Kao R, et al. Ascorbic acid stimulates production of glycosaminoglycans in cultured fibroblasts. Exp Mol Pathol. 1990;53:1–10.

[46] Wei F, Qu C, Song T, et al. Vitamin C treatment promotes mesenchymal stem cell sheet formation and tissue regeneration by elevating telomerase activity. J Cell Physiol. 2012;227:3216–3224.

[47] Wong-In S, Khanhthuyen NT, Siriwatwechakul W, et al. Multilayered mouse preosteoblast MC3T3-E1 sheets harvested from temperature-responsive poly(N-isopropylacrylamide-co-acrylamide) grafted culture surface for cell sheet engineering. J Appl Polym Sci. 2013;129:3061–3069.